



Universiteit
Leiden
The Netherlands

Advancements in minimally invasive image-guided liver therapies

Burgmans, M.C.

Citation

Burgmans, M. C. (2017, October 26). *Advancements in minimally invasive image-guided liver therapies*. Retrieved from <https://hdl.handle.net/1887/54940>

Version: Not Applicable (or Unknown)

License: [Licence agreement concerning inclusion of doctoral thesis in the Institutional Repository of the University of Leiden](#)

Downloaded from: <https://hdl.handle.net/1887/54940>

Note: To cite this publication please use the final published version (if applicable).

Cover Page



Universiteit Leiden



The handle <http://hdl.handle.net/1887/54940> holds various files of this Leiden University dissertation.

Author: Burgmans, M.C.

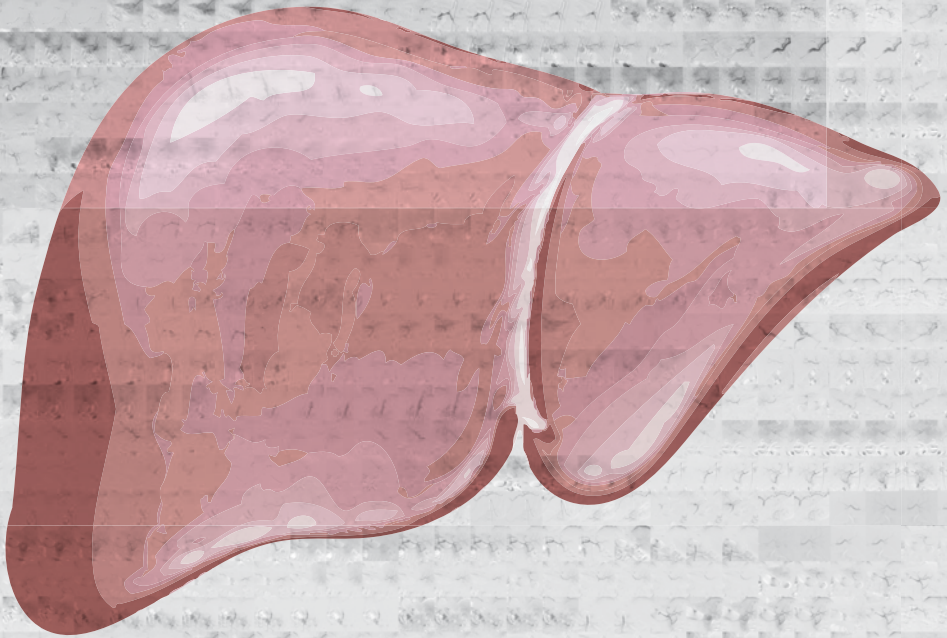
Title: Advancements in minimally invasive image-guided liver therapies

Issue Date: 2017-10-26



Chapter 8

Image-guided personalized predictive dosimetry by artery-specific SPECT/CT partition modeling for safe and effective Y90 radioembolization



Kao YH, Tan AEH, Burgmans MC, Irani FG, Khoo LS, Lo RHG, Tay KH, Tan BS, Chow PKH, Ng DCE, Goh ASW.

J Nucl Med. 2012 Apr;53(4):559-566

ABSTRACT

Purpose

Compliance to radiobiological principles of radionuclide internal dosimetry is fundamental to the success of yttrium-90 (Y90) radioembolization. The artery-specific SPECT/CT partition model is an image-guided personalized predictive dosimetric technique developed by our institution, integrating catheter-directed computed tomography hepatic angiography (CTHA), technetium-99m-macroaggregated albumin (99mTc-MAA) SPECT/CT and partition modeling for unified dosimetry. Catheter-directed CTHA accurately delineates planning target volumes. SPECT/CT tomographically evaluates 99mTc-macroaggregated albumin (99mTc-MAA) hepatic biodistribution. The partition model is validated for Y90 resin microspheres based on Medical Internal Radiation Dosimetry (MIRD) macrodosimetry.

Methods

This was a retrospective analysis of our early clinical outcomes for inoperable hepatocellular carcinoma (HCC). Mapping hepatic angiography was performed according to standard technique with addition of catheter-directed CTHA. 99mTc-MAA planar scintigraphy was used for liver-to-lung shunt estimation, and SPECT/CT for liver dosimetry. Artery-specific SPECT/CT partition modeling was planned by experienced nuclear medicine physicians.

Results

From January to May 2011, 20 arterial territories were treated in 10 HCC patients. Median follow-up was 21 weeks (95% confidence interval (CI), 12-50). When analyzed strictly as brachytherapy, Y90 radioembolization planned by predictive dosimetry achieved index tumor regression in 8 of 8 patients, with median size decrease of 58% (95% CI, 40%-72%). Tumor thrombosis regressed or remained stable in 3 of 4 patients with baseline involvement. Best alphafetoprotein reduction ranged from 32 to 95%. Clinical success was achieved in 7 of 8 patients, including 2 by sub-lesional dosimetry, one of which had radioembolization lobectomy intent. Median predicted mean radiation absorbed doses were 106 Gy (95% CI, 105-146 Gy) to tumor, 27 Gy (95% CI, 22-33 Gy) to non-tumorous liver and 2 Gy (95% CI, 1.3-7.3 Gy) to lungs. Across all patients, tumor, non-tumorous liver and lungs received predicted ≥ 91 Gy, ≤ 51 Gy and ≤ 16 Gy respectively via at least one target arterial territory. No patients developed significant toxicities within 3 months post-radioembolization. The median time to best imaging response was 76 days (95% CI, 55-114 days). Median time to progression and overall survival were not reached. SPECT/CT-derived mean tumor-to-normal liver (T/N) ratios varied widely across all planning target volumes (median 5.4; 95% CI, 4.1-6.7), even within the same patient.

Conclusions

Image-guided personalized predictive dosimetry by artery-specific SPECT/CT partition modeling achieves high clinical success rates for safe and effective Y90 radioembolization.

INTRODUCTION

As a form of arterial territory-specific point-source brachytherapy, yttrium-90 (Y90) radioembolization is always effective when delivered at the right location, in the right dose, and with the right intent. Y90 radioembolization failure is invariably due to one or a combination of these three factors being incorrectly addressed. Responsibility for this triad is shared among the interventional radiologist, the nuclear medicine physician, and the referring clinician. Y90 radioembolization is complex, and a lack of coordinated care risks sub-optimum outcomes.

Contemporary techniques, outcomes, and safety data of Y90 radioembolization are well-described in recent literature (1-8). Disregard for radiobiological principles of arterial territory-specific Y90 radionuclide internal dosimetry risks toxicity and fatality (9-10). Since the 1980s, sectional imaging (e.g. computed tomography) has revolutionized the planning and delivery of external beam radiation therapy (EBRT). However to date, radiation planning for Y90 radioembolization has yet to embrace modern imaging modalities such as catheter-directed CT hepatic arteriography (CTHA) and single photon emission computed tomography with integrated low-dose CT (SPECT/CT).

Catheter-directed CTHA delineates hepatic arterial territorial margins more accurately than digital subtraction angiography (1,11). SPECT/CT is superior to both planar scintigraphy and SPECT for assessing intra-hepatic biodistribution of technetium-99m-macroaggregated albumin (99mTc-MAA), and for estimating the tumor-to-normal liver (T/N) ratio (12-14). The partition model is a validated dosimetric method for Y90 resin microspheres, scientifically superior to the 'body surface area (BSA)' method (5,10).

Accurate assessment of target liver volumes is critical because it directly affects radiation absorbed dose estimates. This is especially important when planning for selective (lobar) or super-selective (segmental or sub-segmental) Y90 radioembolization. Catheter-directed CTHA refers to the acquisition of CT with direct intraarterial injection of dilute contrast media through an angiographic catheter or microcatheter introduced into a hepatic lobar, segmental or sub-segmental artery via a percutaneous transfemoral arterial puncture (1,11). This provides superior delineation of arterial territories compared to digital subtraction angiography, enabling accurate estimation of artery-specific perfused liver volumes (1,11). Conventional Y90 radioembolization is planned on the interventional radiologists' assessment of each patient's vascular anatomy (15). However, estimation of the perfused liver volume can be challenging. Hepatic vascular anatomy has many variations (13,15-16). A main hepatic artery may supply several liver segments via its branches; conversely a single segment may be supplied by more than one arterial

branch. Couinaud segments may be distorted by large tumors, previous liver surgery or locoregional therapy – for example, ablation cavities. Aberrant arteries due to neoplastic recruitment from extrahepatic sources further complicate hepatic vascular anatomy. These factors make it difficult to reliably estimate the target volume of a diseased liver based on digital subtraction angiography alone.

This problem may be overcome by catheter-directed CTHA. With the catheter tip placed in the target artery, CT performed at the time of intra-arterial contrast injection provides superior delineation of the perfused liver volume, as compared to that shown under digital subtraction angiography. Each 'run' of catheter-directed CTHA is specific for its catheter tip position. The use of catheter-directed CTHA shifts the planning emphasis away from a conventional lobe or segment-based approach to a more patient-specific arterial territory-based approach. Catheter-directed CTHA accurately delineates each target arterial territory regardless of arterial anatomy, variant vasculature, or tissue distortion by tumor, surgery, or locally ablative treatments.

The role of SPECT/CT in diagnostic imaging and internal dosimetry is well established in nuclear medicine (17-18). In the context of Y90 radioembolization, 99mTc-MAA SPECT/CT for preradioembolization assessment has a higher detection rate for extrahepatic radiotracer activity and has greater impact on therapy planning compared to that under planar scintigraphy (14,19-20). Hepatic intraarterial 99mTc-MAA scintigraphy is a validated means of simulating the Y90 radioembolization therapy field (13-14). SPECT/CT-based dosimetry is superior to planar scintigraphy by tomographically resolving overlapping radiotracer activity, evaluating heterogeneous radiotracer uptake and detecting activity in small lesions (12,14,17). Phantom studies have shown that 99mTc-MAA SPECT/CT volume measurements are accurate and reproducible (13). To date, no standardized technique exists for the calculation of SPECT/CT-based T/N ratios, although several methods have been described (21-23).

The partition model was developed and validated for Y90 resin microspheres by Ho et al. in the 1990s (24-25). It is one of several methods recommended by the manufacturer of Y90 resin microspheres to calculate the desired Y90 activity (26). Based on Medical Internal Radiation Dosimetry (MIRD) macrodosimetry, it partitions the lungs, tumor, and non-tumorous liver into separate compartments for radiation dose modeling (24,26). This model surpasses the commonly used BSA method by incorporating absolute tissue masses and patient-specific mean T/N ratios for personalized and scientifically sound estimates of mean radiation absorbed doses to each tissue compartment (5,10,27). Technical differences between BSA methodology and partition modeling discussed elsewhere, along with limitations and clinical implications (10).

The artery-specific SPECT/CT partition model is a unified technique of personalized predictive dosimetry developed by our institution for Y90 radioembolization using resin microspheres. It integrates catheter-directed CTHA, 99mTc-MAA SPECT/CT and partition modeling for improved predictive radionuclide dosimetry. Its fundamental premise is to derive more accurate estimates of tissue masses and mean T/N ratios to optimize partition modeling. The underlying principles and limitations of MIRD macrodosimetry remain unchanged. Through the use of artery-specific SPECT/CT partition modeling, predicted mean radiation absorbed doses specific to target arterial territories are independently calculated and physician-adjusted according to patient-specific circumstances (e.g. mean T/N ratio, liver-to-lung shunt, liver reserve, prognosis, treatment intent and potential treatment benefit). The overall process yields a personalized image-guided predictive radiation plan for safe and effective Y90 radioembolization. This report provides a technical overview of this integrated dosimetric technique and details our early clinical outcomes in patients with inoperable hepatocellular carcinoma (HCC).

METHODS

Patients

The institutional review board waived the need to obtain informed consent for this retrospective study. The technique for using artery-specific SPECT/CT partition modeling to plan Y90 radioembolization was implemented at our institution as a routine clinical service in January 2011. Five months post-implementation, we had treated 22 patients with inoperable HCC. Of these, 10 patients were embargoed under an ongoing clinical trial. Two patients were planned by BSA methodology due to morphologically diffuse and infiltrative tumors that were below 99mTc-MAA SPECT/CT resolution for reliable regions-of-interest (ROI) contouring. Both these patients were excluded (10). Treatment of the remaining 10 consecutive patients was planned by artery-specific SPECT/CT partition modeling, and these patients were eligible for inclusion into this report. Retrospective review of hospital medical records was performed for these 10 patients until August 2011, the time at which the manuscript was prepared.

Patient and baseline disease characteristics were highly heterogeneous (Tables 1 and 2).

Median age was 59 years (range 48-65 years). There were 8 men and 2 women. Seven patients had chronic viral hepatitis. Five patients received prior therapy for HCC, including 2 with previous Y90 radioembolization planned by conventional planar partition modeling. Eight patients were Child-Pugh A; the remainder were Child-Pugh B. *Tumor*

Table 1. Patient characteristics

Patient No.	Age	Sex	Tumor	Risk factor	Previous Treatment	ECOG	Child-Pugh
1	58	M	HCC	HCV	Segmentectomy; sorafenib	1-2	A
2	63	M	HCC	HBV	Y90 RE; segmentectomy	0	A
3	61	F	HCC	Cryptogenic	No	3	A
4	48	M	HCC	HBV	RFA	1-2	B
5	60	M	HCC	Cryptogenic	No	0	A
6	56	M	HCC	HBV	Right hemi-hepatectomy; TACE	0	A
7	61	F	HCC	Cryptogenic	Y90 RE	1-2	A
8	65	M	HCC	HCV	No	0	B
9	56	M	HCC	HBV	No	0	A
10	52	M	HCC	HCV	No	0	A

HCC: hepatocellular carcinoma; HBV: chronic hepatitis B; HCV: chronic hepatitis C; ECOG: Eastern cooperative oncology group performance status; PV: portal vein; Y90 RE: Y90 radioembolization; RFA: radiofrequency ablation; TACE: transarterial chemoembolization

Table 2. Disease characteristics

Patient No.	UNOS T-stage	BCLC	Tumor extent	Vascular invasion	Site of hepatic intra-arterial 99mTc-MAA injection
1	T4b	C	Bilobar; infiltrative	Branch PV	Right; left *
2	rT2	A	Solitary recurrence at segment IV resection margin	No	Right; left *
3	T3	D	Central large dominant tumor; smaller satellite lesions	No	Right; left *
4	T4b	C	Right lobe; multifocal	Branch PV	Superior branch of right; posterior branch of right †
5	T4b	C	Bilobar; multifocal; subcentimeter lesions present	Branch PV	Right; accessory right; left *
6	T4b	B	Bilobar; multifocal; subcentimeter lesions present	No	Right; left *
7	T4a	B	Right lobe; large necrotic tumor; satellite lesions with ill-defined margins	No	Right; middle †
8	T4a	B	Bilobar; multifocal; subcentimeter lesions present	No	Right; middle; left *
9	T4b	C	Bilobar; multifocal; subcentimeter lesions present	Branch PV	Proper *
10	T4b	C	Large right lobe tumor with ill-defined margins; subcentimeter lesion present	Branch and main PV; right hepatic vein	Right †

UNOS: United Network for Organ Sharing staging system, all patients are N0 M0; BCLC: Barcelona Clinic Liver Cancer staging system; PV: portal vein; * Whole-liver 99mTc-MAA injection; † Selective lobar/segmental 99mTc-MAA injection

extent varied widely across all patients and were mostly bilobar and multifocal. Eight patients had T4 disease by the United Network for Organ Sharing (UNOS) staging system; none had nodal or distant metastases. Classification by the Barcelona Clinic Liver Cancer (BCLC) staging system was: 1 BCLC A; 3 BCLC B; 5 BCLC C; 1 BCLC D. Five patients had tumor vascular involvement.

Technique overview

Mapping hepatic angiography and ^{99m}Tc -MAA injection were performed according to standard technique (1, 15). Prophylactic coil embolization of vessels at risk was performed either at mapping hepatic angiography or at ^{90}Y radioembolization, at the discretion of the interventional radiologist. The catheter tip position for ^{99m}Tc -MAA injection was decided in consensus between the interventional radiologist and nuclear medicine physician during mapping hepatic angiography. ^{99m}Tc -MAA was slowly hand-injected non-selectively (whole liver), selectively (lobar) or super-selectively (segmental or sub-segmental) depending on patient-specific circumstances. Patients were immediately transferred to the gamma camera suite for planar liver-to-lung shunt scintigraphy and SPECT/CT of the abdomen.

The following describes the essence of the technique of artery-specific SPECT/CT partition modeling. Catheter-directed CTHA guided volumes-of-interest (VOI) delineation on ^{99m}Tc -MAA SPECT/CT to obtain arterial territory-specific tissue volumes and SPECT/CT-based mean T/N ratio estimates for improved partition modeling. The term *planning target volume* is used, adapted from EBRT. All treatments were planned by a team of experienced nuclear medicine physicians, and the final prescribed mean radiation absorbed doses were guided by published dose-response relationships (5). By partition modeling, the nuclear medicine physician had full control over predicted radiation absorbed dose estimates to tumor, non-tumorous liver and lungs within each planning target volume. The overall dosimetric aim was to balance the desired mean tumor radiation absorbed dose with collateral radiation injury, in accordance to the treatment intent.

^{90}Y radioembolization was performed using resin microspheres (SIR-Spheres[®], Sirtex Medical Limited, New South Wales, Australia) within 2 weeks of mapping hepatic angiography. Catheter tip placement was the same as that of the ^{99m}Tc -MAA injections. All patients received prophylactic omeprazole, 20mg, twice daily prior to ^{90}Y radioembolization and this treatment continued for at least 6 weeks after radioembolization. In accord with our institutional protocol, after ^{90}Y radioembolization all patients were observed overnight and discharged after bremsstrahlung planar scintigraphy of the lung and SPECT/CT of the abdomen the following day.

Terms and definitions

Postradioembolization bremsstrahlung SPECT/CT of the abdomen was used to determine technical success. Technical success was achieved when all targeted tumors within planning target volumes showed satisfactory bremsstrahlung activity by visual assessment, in keeping with the radiation plan (28). The success of the technique was considered indeterminate when planning target volumes included subcentimeter tumors or tumors with ill-defined margins (e.g. infiltrative HCC), below bremsstrahlung SPECT/CT spatial resolution. A technical failure occurred when targeted tumors did not exhibit visually detectable focal bremsstrahlung activity, analogous to a geographical miss in the context of EBRT.

Clinical and biochemical toxicities within 3 months after radioembolization were classified according to Common Terminology Criteria for Adverse Events (CTCAE v4.03) (28-29). The nadir in serum alphafetoprotein at any time post-radioembolization indicated the best biochemical response.

To evaluate the effectiveness of Y90 radioembolization strictly as a form of brachytherapy delivered at a single time-point, the best imaging response was defined as the greatest change in size of the targeted index (largest) tumor between baseline and follow-up diagnostic sectional imaging. Clinical success was defined as any degree of regression of targeted tumors on follow-up diagnostic sectional imaging within planning target volumes, regardless of new tumors appearing within or outside planning target volumes (28).

Overall response by Response Evaluation Criteria in Solid Tumors version 1.1 (RECIST 1.1), World Health Organization (WHO), and 2-D European Association for the Study of the Liver (2D-EASL) guidelines were used to evaluate Y90 radioembolization as a part of comprehensive multi-modality therapy for inoperable HCC, without regard to planning target volumes (28,30).

Statistical methods

Data are presented as median and 95% confidence intervals (CI), where applicable. Using Bland-Altman analysis, the total desired Y90 activities calculated by artery-specific SPECT/CT partition modeling were compared to that hypothetically derived by BSA methodology. The intra-class correlation coefficient (ICC) was calculated with values 0.8 or more considered excellent; 0.6-0.8, good; 0.4-0.6, moderate; and less than 0.4, poor. Statistical analysis was performed on Microsoft® Office Excel 2003 (Microsoft Corporation) and SPSS version 17.0 (SPSS Inc., Chicago, USA).

RESULTS

The artery-specific SPECT/CT dosimetric plans of all 10 patients are summarized in Table 3. There were a total of 20 radiation plans across 10 patients i.e. one planning target volume per target arterial territory. Two patients underwent Y90 radioembolization in a single arterial territory, 6 patients in 2 arterial territories and 2 patients in 3 arterial territories (Figure 1).

Sublesional dosimetry was performed in 2 patients; 1 of which was planned with radioembolization lobectomy intent (Figures 2-3). Four patients underwent prophylactic coil embolization of arteries at risk: 3 gastroduodenal; 2 accessory left gastric; 2 right gastric; 1 right inferior phrenic; 1 falciform; 1 pancreatico-duodenal arcade. Technical success was achieved in 2 of 10, indeterminate in 7 of 10, and technical failure in 1 of 10 patients. Patient 8 was classified as a technical failure due to the absence of visually detectable focal bremsstrahlung activity in a targeted caudate tumor.

Median predicted mean radiation absorbed doses by artery-specific SPECT/CT partition modeling were 106 Gy (95% CI, 105-146 Gy) to tumor, 27 Gy (95% CI, 22-33 Gy) to non-tumorous liver and 2 Gy (95% CI, 1.3-7.3 Gy) to lungs. Across all patients, tumor, non-tumorous liver and lungs were predicted to have received ≥ 91 Gy, ≤ 51 Gy and ≤ 16 Gy respectively to at least one target arterial territory. The median artery-specific tumor and non-tumorous liver masses were 156 g (95% CI, 117-436 g) and 752 g (95% CI, 513-833 g) respectively. The median liver-to-lung shunt estimated by planar 99mTc-MAA scintigraphy was 5.4% (95% CI, 4.3%-9.0%). The median Y90 activity injected into an arterial territory was 0.6 GBq (95% CI, 0.7-1.3 GBq). Patient 2 received a mean radiation absorbed dose of 93 Gy to the left lobe nontumorous liver for Y90 radioembolization lobectomy (Table 3; Fig. 2). There was good tumor response together with slow progressive atrophy of the left lobe 6 months post-radioembolization, in keeping with the dosimetric intent. The right lobe volume, which received a mean radiation absorbed dose of 27 Gy to non-tumorous liver, remained stable over time (Figure 3).

SPECT/CT-based mean T/N ratios varied widely across all planning target volumes (median 5.4; 95% CI, 4.1-6.7), and even within the same patient (median intra-patient difference 1.9; 95% CI, 1.1-2.5). We could not find any predictive relationship between mean T/N ratios and liver tissue masses. In a sub-analysis, the total desired Y90 activities calculated by artery-specific SPECT/CT partition modeling were compared to that hypothetically derived by BSA methodology. Bland-Altman analysis (Figure 4) showed a wide 95% limit of agreement ranging from -1.12 to +1.41, with only moderate correlation (ICC 0.59; 95% CI, -0.71 to 0.90).

Table 3. Dosimetric data by artery-specific SPECT/CT partition modeling

Pt No.	¹³¹ I Y90 RE radiation dose	1	Planning target volume	2	Planning target volume	3	Planning target volume	Artery prophylactic coil embolization	Liver-lung shunt, Gy	Total injected Y90 activity	Technical success*
1	N/A	Right hepatic artery T/N ratio 5.7 Tumor mass 259g Tumor dose 171Gy Liver mass 920g Liver dose 30Gy Y90 activity 1.6GBq	Left hepatic artery T/N ratio 8.1 Tumor mass 46g Tumor dose 177Gy Liver mass 833g Liver dose 22Gy Y90 activity 0.5GBq	N/A	No	8.3% 5Gy	2.1GBq	Indeterminate; ill-defined tumor margins †			
2	Liver 70Gy; Lung 9Gy ‡	Right hepatic artery T/N ratio 6.1 Tumor mass 7g Tumor dose 164Gy Liver mass 782g Liver dose 27Gy Y90 activity 0.4GBq	Left hepatic artery § T/N ratio 1.4 Tumor mass 28g Tumor dose 133Gy Liver mass 256g Liver dose 93Gy Y90 activity 0.6GBq	N/A	No	4.5% 1Gy	1.0GBq	Yes			
3	N/A	Right hepatic artery T/N ratio 6.5 Tumor mass 410g Tumor dose 92Gy Liver mass 983g Liver dose 14Gy Y90 activity 1.0GBq	Left hepatic artery T/N ratio 4.6 Tumor mass 172g Tumor dose 59Gy Liver mass 752g Liver dose 13Gy Y90 activity 0.4GBq	N/A	Accessory/left gastric; gastro-duodenal ¶	4.6% 2Gy	1.4GBq	Indeterminate; subcentimeter lesions ¶			
4	N/A	Right hepatic artery (superior branch) T/N ratio 8.1 Tumor mass 58g Tumor dose 241Gy Liver mass 189g Liver dose 30Gy Y90 activity 0.4GBq	Right hepatic artery (posterior branch) T/N ratio 8.4 Tumor mass 484g Tumor dose 176Gy Liver mass 825g Liver dose 21Gy Y90 activity 2.2GBq	N/A	No	10.3% 9Gy	2.6GBq	Yes			

Table 3. Dosimetric data by artery-specific SPECT/CT partition modeling (continued)

Pt No.	¹²⁵ I Y90 RE radiation dose	1	2	3	Artery prophylactic coil embolization	Liver-lung shunt, Gy	Total injected Y90 activity	Technical success*
5	N/A	<u>Right hepatic artery</u> T/N ratio 5.2 Tumor mass 337g Tumor dose 135Gy Liver mass 247g Liver dose 26Gy Y90 activity 1.1GBq	<u>Accessory right hepatic artery</u> T/N ratio 3.1 Tumor mass 730g Tumor dose 87Gy Liver mass 423g Liver dose 28Gy Y90 activity 1.5GBq	<u>Left hepatic artery</u> T/N ratio 2.3 Tumor mass 12g Tumor dose 106Gy Liver mass 595g Liver dose 47Gy Y90 activity 0.6GBq	No	3.5% 2Gy	3.2GBq	Indeterminate; subcentimeter lesions ¶
6	N/A	<u>Right hepatic artery</u> T/N ratio 5.6 Tumor mass 27g Tumor dose 151Gy Liver mass 460g Liver dose 27Gy Y90 activity 0.4GBq	<u>Left hepatic artery</u> T/N ratio 7.6 Tumor mass 40g Tumor dose 152Gy Liver mass 1196g Liver dose 20Gy Y90 activity 0.6GBq	N/A	No	8.4% 2Gy	1.0GBq	Indeterminate; subcentimeter lesions ¶
7	Liver 40Gy; Lung 10Gy †	<u>Right hepatic artery</u> T/N ratio 2.1 Tumor mass 156g Tumor dose 106Gy Liver mass 363g Liver dose 51Gy Y90 activity 0.7GBq	<u>Middle hepatic artery</u> T/N ratio 1.7 Tumor mass 12g Tumor dose 85Gy Liver mass 252g Liver dose 51Gy Y90 activity 0.3GBq	N/A	Right inferior phrenic; falciform ¶¶	4.3% 1Gy	1.0GBq	Indeterminate; ill-defined tumor margins †

Table 3. Dosimetric data by artery-specific SPECT/CT partition modeling (continued)

Pt No.	¹³¹ Y90 RE radiation dose	1 Planning target volume	2 Planning target volume	3 Planning target volume	Artery prophylactic coil embolization	Liver-lung shunt, Gy	Total injected Y90 activity	Technical success*
8	N/A	Right hepatic artery T/N ratio 2.4 Tumor mass 266g Tumor dose 91Gy Liver mass 1465g Liver dose 38Gy Y90 activity 1.6GBq	Left hepatic artery T/N ratio 4.3 Tumor mass 23g Tumor dose 107Gy Liver mass 1044g Liver dose 25Gy Y90 activity 0.6GBq	Middle hepatic artery T/N ratio 3.2 Tumor mass 10g Tumor dose 95Gy Liver mass 356g Liver dose 30Gy Y90 activity 0.2GBq	Right gastric; gastro-duodenal #	6.1% 3Gy	2.4GBq	No; Non-implantation in caudate tumor
9	N/A	Proper hepatic artery T/N ratio 11.5 Tumor mass 1252g Tumor dose 97Gy Liver mass 755g Liver dose 8Gy Y90 activity 2.6GBq	N/A	N/A	Accessory left gastric ; right gastric ; gastro-duodenal #; pancreatico-duodenal arcade #	1.7% 2Gy	2.6GBq	Indeterminate; subcentimeter lesions ¶
10	N/A	Right hepatic artery T/N ratio 10.6 Tumor mass 955g Tumor dose 97Gy Liver mass 350g Liver dose 9Gy Y90 activity 2.3GBq	N/A	N/A	No	14.5% 16Gy	2.3GBq	Indeterminate; ill-defined tumor margins; subcentimeter lesions † ¶

RE: Y90 radioembolization; T/N ratio: tumor-to-normal liver ratio; N/A: not applicable; * Technical success assessed by bremsstrahlung SPECT/CT; † Dose; ‡ predicted mean radiation absorbed dose in Gy; † Ill-defined tumor margins cannot be reliably assessed by bremsstrahlung SPECT/CT; ‡ Planned by planar partition modeling; § Planned by sub-lesional dosimetry with radiation lobectomy intent to the left hepatic arterial territory; || Coil embolization at time of mapping hepatic angiography; ¶ Subcentimeter lesions are below bremsstrahlung SPECT/CT spatial resolution; # Coil embolization at time of Y90 radioembolization

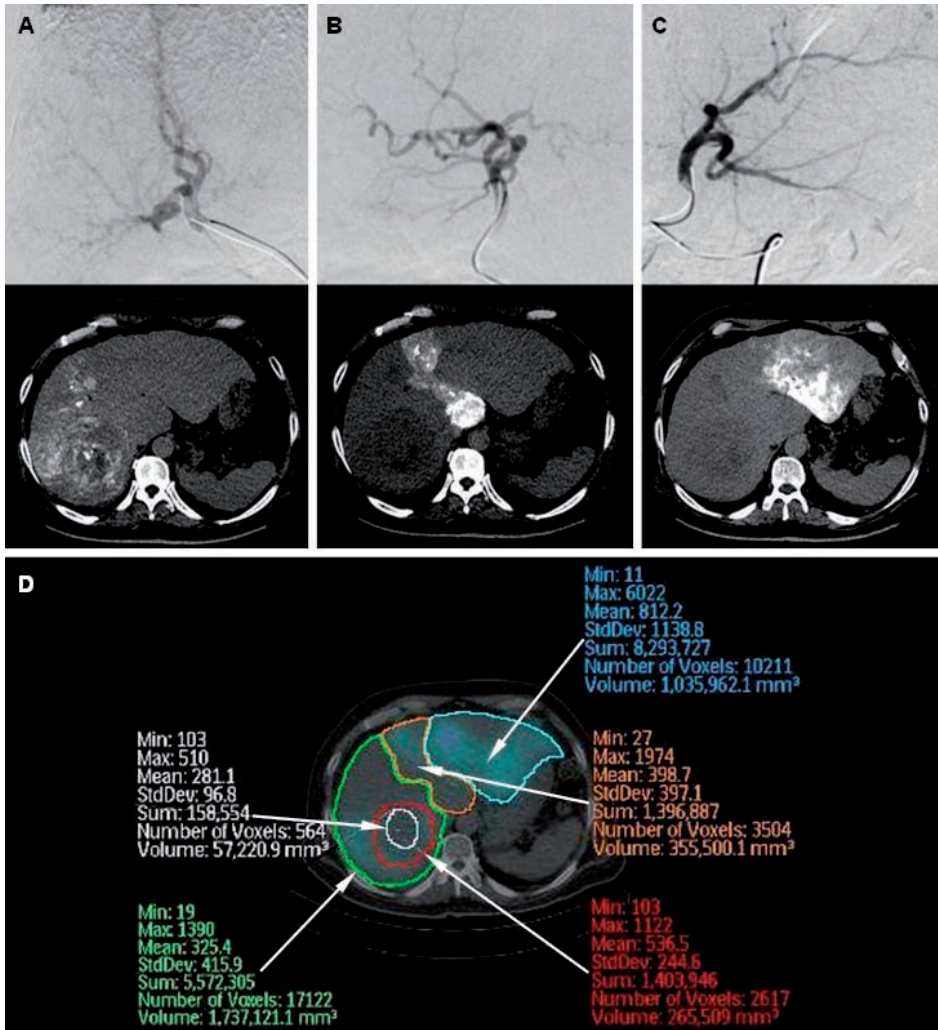


Figure 1. Example of artery-specific SPECT/CT partition modeling of 3 arterial territories. A liver with multifocal HCC supplied by the right (A), middle (B) and left (C) hepatic arteries is depicted here in digital subtraction angiography and catheter-directed CTHA respectively. Regions-of-interest (ROI) are drawn on ^{99m}Tc-MAA SPECT/CT transaxial slices representing the left (D, blue ROI), middle (D, orange ROI) and right (D, green ROI) hepatic artery planning target volumes, the implanted tumor (D, red ROI) and necrotic tumor (D, white ROI).

Y90 radioembolization was well tolerated in all patients. None developed postradioembolization syndrome. All patients were ambulating freely by the next day and discharged within 24 hours post-radioembolization. In 8 patients, serum bilirubin, albumin, and alanine transaminase (ALT) were measured within 24 hours post-radioembolization; none developed significant biochemical toxicities.

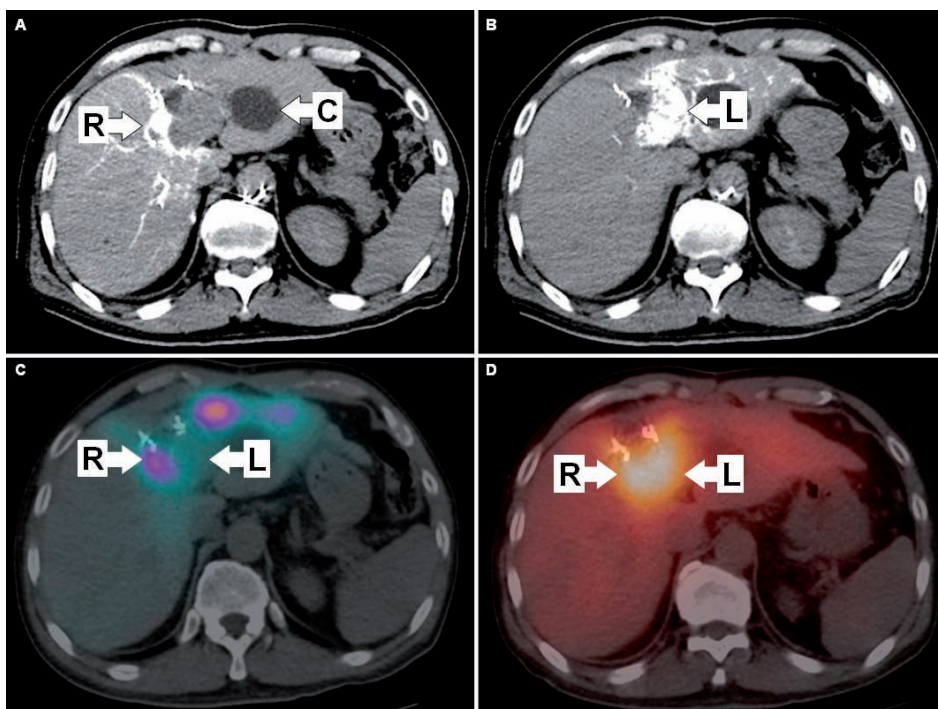


Figure 2. Patient 2: Example of sub-lesional dosimetry with left radioembolization lobectomy intent. The patient had recurrent HCC at the segment IV resection margin. Left lobe hypodensity is a cyst (A, 'C'). The tumor was supplied by the right and left hepatic arteries. Catheter-directed CTHA depicts the planning target volumes of the right (A) and left (B) hepatic arteries, dividing the dosimetric plan into two independent halves for sub-lesional dosimetry. ^{99m}Tc -MAA SPECT/CT showed good T/N ratio (6.1) of the lateral tumor portion supplied by the right hepatic artery (C, 'R'), but poor T/N ratio (1.4) of the medial tumor portion supplied by the left hepatic artery (C, 'L'). The dosimetric plan of the left hepatic artery planning target volume was deliberately escalated beyond safe limits to achieve a predicted mean radiation absorbed dose of 133 Gy to tumor and 93 Gy to non-tumorous liver, where progressive atrophy of the left lobe was the anticipated collateral effect i.e. left radioembolization lobectomy intent. Post-radioembolization bremsstrahlung SPECT/CT showed good tumoral activity in both lateral (D, 'R') and medial (D, 'L') tumor portions, indicating technical success.

At the time of this report, follow-up data was available for 8 patients. The median follow-up duration was 21 weeks (95% CI, 12-50 weeks). The other 2 patients were non-residents, returned to their home country and were lost to follow-up. Patient 3 was excluded from biochemical and survival analysis due to confounding medical issues, but was included in imaging analysis.

With the exception of Patient 3, all 7 other patients remained clinically well. None developed gastrointestinal complications or radiation pneumonitis. There were no biochemical toxicities beyond CTCAE Grade 2 within 3 months postradioembolization. Postradioembolization serum alphafetoprotein was available in 5 patients. There was an

interval decrease in alphafetoprotein in 3 patients, ranging from 32 to 95%. The remaining 2 patients had normal baseline alphafetoprotein levels, which remained un-elevated on follow-up.

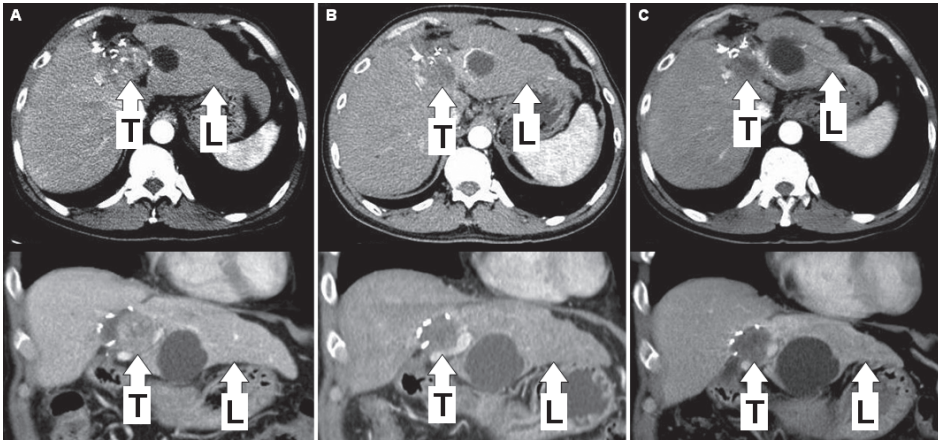


Figure 3. Patient 2: Baseline triphasic CT liver shows the recurrent HCC at the segment IV resection margin (A). Follow-up triphasic CT liver at three (B) and six (C) months post-radioembolization showed good tumor ('T'; 133 Gy) response with progressive atrophy of the left lobe ('L'; 93 Gy), in keeping with left radioembolization lobectomy intent. Right lobe volume (27 Gy) remained stable.

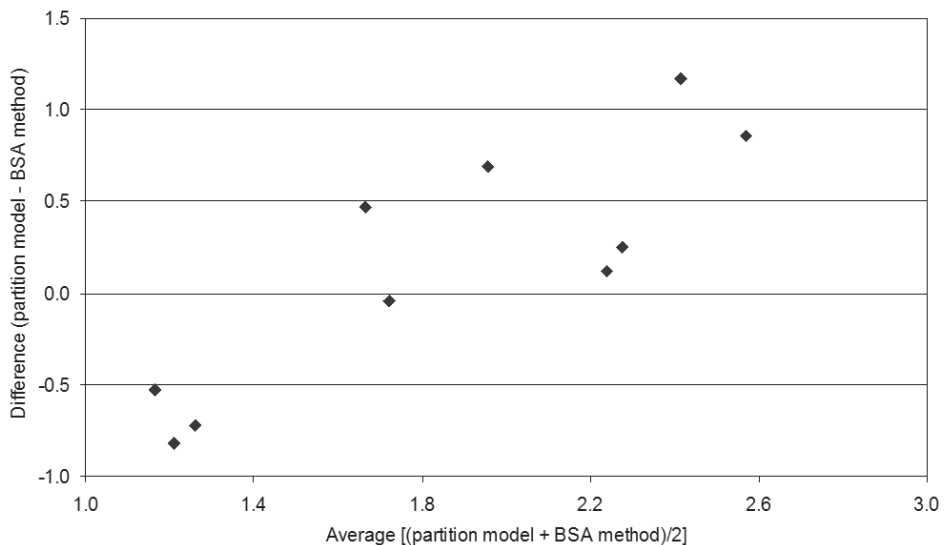


Figure 4. Bland-Altman plot of Y90 activities derived by artery-specific SPECT/CT partition modeling versus that hypothetically derived by body surface area (BSA) methodology.

Postradioembolization best imaging response was available in 8 patients. Median time-to-best imaging response was 76 days (11 weeks; 95% CI 55-114 days). When Y90 radioembolization was analyzed strictly as a brachytherapy, all 8 of 8 patients showed regression of the index tumor, with a median size decrease of 58% (95% CI, 40%-72%). None developed new tumors within planning target volumes. Seven of 8 patients achieved clinical success at the time of best imaging response. Patient 1 was a case of infiltrative HCC classified as clinical failure due to progression of existing portal vein tumor thrombosis despite significant regression of the index tumor. Otherwise, tumor thrombosis regressed or remained stable in 3 of 4 patients with baseline tumor vascular involvement.

At the time of best imaging response, extrahepatic metastases were discovered in 3 of 8 patients, involving the lungs and adrenal gland. When Y90 radioembolization was analyzed as part of a comprehensive multi-modality treatment plan, partial response was achieved in 3 of 8, stable disease in 1 of 8, and progressive disease in 4 of 8 patients; consistent across all three classifications (RECIST 1.1, WHO and 2D-EASL). Median imaging time-to-progression (TTP) and median overall survival were not reached at the time of this report. Patient 1 died 13 weeks postradioembolization and had an overall survival of 95 weeks (22 months) under comprehensive multi-modality care; all 7 other patients are still alive.

DISCUSSION

The aim of personalized predictive dosimetry is to guide decisions on radionuclide therapy in order to avoid the use of futile therapy and achieve the maximum tumor radiation absorbed dose while minimizing collateral radiation injury to normal tissue.

Precise radionuclide predictive dosimetry has the potential to yield many benefits for cancer therapy, and the need to further research into internal dosimetry has recently been emphasized (31). To our knowledge, the artery-specific SPECT/CT partition model is the first to integrate catheter-directed CTHA, ^{99m}Tc-MAA SPECT/CT and partition modeling (MIRD) into a unified, accurate, and practical form of image-guided personalized predictive dosimetry for Y90 radioembolization.

Our results show that a 100% tumor response rate can be achieved when the predicted mean tumor radiation absorbed dose was at least 91 Gy to a planning target volume. There were no significant toxicities with predicted mean radiation absorbed doses to non-tumorous liver and lungs of ≤ 51 Gy and ≤ 16 Gy, respectively. This highlights the

power of predictive radionuclide dosimetry to achieve desired outcomes when planned in accordance to dose-response relationships. The capability of artery-specific SPECT/CT partition modeling is best exemplified by patient 2, in whom sub-lesional dosimetry was successfully planned with Y90 radioembolization lobectomy intent (Figs. 2-3).

Y90 radioembolization is point-source, continuous low dose-rate brachytherapy delivered at a single time-point. Hence, its true therapeutic efficacy can only be revealed by analyzing outcomes in the context of planning target volumes and technical success. Therefore, postradioembolization appearance of new tumors within a planning target volume should not be misconstrued as clinical failure. Such lesions may represent new metastases, pre-existing micro-metastases that have enlarged, or *de novo* tumors arising from cirrhotic liver; all of which have little or no bearing on Y90 radioembolization as brachytherapy delivered at a single time-point. It follows that when applying standard response evaluation criterion (e.g. RECIST), which takes into account new tumors and distant metastases, one should analyze Y90 radioembolization brachytherapy as part of comprehensive multi-modality care and not in isolation.

The application of Y90 radioembolization without due regard for radiobiological principles is akin to flying an aircraft without guidance from air traffic control. Since most patients with inoperable HCC have limited prognosis, Y90 radioembolization should be carefully planned using scientifically sound methods (e.g. MIRD) to achieve the maximum desired effect for optimal, personalized cancer therapy. Our dosimetric data showed wide inter- and intra-patient variations in SPECT/CT-based mean T/N ratios (Table 3), emphasizing the importance of having a personalized dosimetric approach to Y90 radioembolization. The assumption of a standard T/N ratio for the sake of dosimetric simplification may result in over- or undertreatment, and confounds data analyses because reliable dose-response relationships cannot be established or verified (10). Despite its popularity, the BSA method has questionable radiobiological basis and is scientifically inferior to MIRD methodology (5,10). One must be cognizant that the BSA method was first published by van Hazel et al. for whole-liver Y90 radioembolization to previously untreated colorectal liver metastasis, not HCC (32). These patients did not have chronic liver disease, prior liver resection, local ablation, or selective/super-selective Y90 radioembolization. Furthermore, colorectal liver metastases are rarely bulky enough to distort liver anatomy. These features are often present in HCC, and therefore they cast doubt on the validity, safety, and efficacy of the BSA methodology for use in HCC. Our data showing a lack of agreement in total Y90 activities derived by artery-specific SPECT/CT partition modeling versus BSA method is further evidence against the routine use of BSA methodology (Figure 4).

In this report, postradioembolization bremsstrahlung SPECT/CT was used to determine technical success. This was indeterminate in 7 of 10 patients, all of whom have either sub-centimeter tumors or tumors with ill-defined margins. This finding highlights the low spatial resolution of bremsstrahlung SPECT/CT as a technical limitation by indirectly imaging Y90 biodistribution using scatter radiation. It may be possible for positron emission tomography to overcome this limitation by co-incidence imaging of yttrium-90 internal pair production (33). This is currently under investigation at our institution.

Y90 microspheres once implanted, remain permanently in place and decays to infinity in situ. This simplifies the dosimetric process because time-activity curves need not be obtained, unlike systemic radionuclide therapy. Future Y90 radioembolization dosimetric techniques must improve accuracy in several areas: delineation of arterial territory target volumes, microparticle simulation and biodistribution assessment, and predictive radiation dose-response modeling. For example, future development of positron-labeled microspheres in place of ^{99m}Tc -MAA may increase the accuracy of liver-to-lung shunt calculation, simulation of hepatic microsphere biodistribution, and improve predictive radiation modeling by voxel- or Monte-Carlo-based techniques (34-35). Y90 radioembolization will also benefit from a wealth of experience if EBRT radiobiologic models (e.g. linear quadratic model, normal tissue complication probability model) and radiation planning techniques (e.g. dose-volume histogram) can be meaningfully translated into radionuclide dosimetry models (e.g. MIRD) and vice versa. Application of the biologically effective dose (BED) concept into Y90 radioembolization dosimetry may achieve this aim (36).

In conclusion, compliance to radiobiological principles of radionuclide internal dosimetry is fundamental to Y90 radioembolization success. Image-guided personalized predictive dosimetry by artery-specific SPECT/CT partition modeling achieves high clinical success rates for safe and effective Y90 radioembolization.

REFERENCES

1. Salem R, Lewandowski RJ, Sato KT, et al. Technical aspects of radioembolization with Y90 microspheres. *Tech Vasc Interv Radiol.* 2007;10:12-29.
2. Gaba RC, Lewandowski RJ, Kulik LM, et al. Radiation lobectomy: preliminary findings of hepatic volumetric response to lobar yttrium-90 radioembolization. *Ann Surg Oncol.* 2009;16:1587-1596.
3. Riaz A, Lewandowski RJ, Kulik LM, et al. Complications following radioembolization with yttrium-90 microspheres: a comprehensive literature review. *J Vasc Interv Radiol.* 2009;20:1121-1130.
4. Ahmadzadehfar H, Biersack HJ, Ezziddin S. Radioembolization of liver tumors with yttrium-90 microspheres. *Semin Nucl Med.* 2010;40:105-121.
5. Lau WY, Kennedy AS, Kim YH, et al. Patient selection and activity planning guide for selective internal radiotherapy with yttrium-90 resin microspheres. *Int J Radiat Oncol Biol Phys.* 2010 Jan 1;82(1):401-407.
6. Salem R, Lewandowski RJ, Mulcahy MF, et al. Radioembolization for hepatocellular carcinoma using Yttrium-90 microspheres: a comprehensive report of long-term outcomes. *Gastroenterology.* 2010;138:52-64.
7. Wang SC, Bester L, Burnes JP, et al. Clinical care and technical recommendations for Y90ttrium microsphere treatment of liver cancer. *J Med Imaging Radiat Oncol.* 2010;54:178-187.
8. Riaz A, Gates VL, Atassi B, et al. Radiation segmentectomy: a novel approach to increase safety and efficacy of radioembolization. *Int J Radiat Oncol Biol Phys.* 2011;79:163-171.
9. Jakobs TF, Hoffmann RT, Fischer T, et al. Radioembolization in patients with hepatic metastases from breast cancer. *J Vasc Interv Radiol.* 2008;19:683-690.
10. Kao YH, Tan EH, Ng CE, Goh SW. Clinical implications of the body surface area method versus partition model dosimetry for yttrium-90 radioembolization using resin microspheres: a technical review. *Ann Nucl Med.* 2011;25:455-461.
11. Rhee TK, Omary RA, Gates V, et al. The effect of catheter-directed CT angiography on yttrium-90 radioembolization treatment of hepatocellular carcinoma. *J Vasc Interv Radiol.* 2005;16:1085-1089.
12. Pereira JM, Stabin MG, Lima FR, Guimarães MI, Forrester JW. Image quantification for radiation dose calculations - limitations and uncertainties. *Health Phys.* 2010;99:688-701.
13. Garin E, Rolland Y, Lenoir L, et al. Utility of quantitative Tc-MAA SPECT/CT for yttrium-labelled microsphere treatment planning: calculating vascularized hepatic volume and dosimetric approach. *Int J Mol Imaging.* July 28, 2011 (Epub ahead of print).
14. Kao YH, Tan EH, Teo TK, Ng CE, Goh SW. Imaging discordance between hepatic angiography versus Tc-99m-MAA SPECT/CT: a case series, technical discussion and clinical implications. *Ann Nucl Med.* 2011 Nov;25(9):669-676.
15. Salem R, Thurston KG. Radioembolization with 90Yttrium microspheres: a state-of-the-art brachytherapy treatment for primary and secondary liver malignancies. Part 1: Technical and methodologic considerations. *J Vasc Interv Radiol.* 2006;17:1251-1278.
16. Covey AM, Brody LA, Maluccio MA, Getrajdman GI, Brown KT. Variant hepatic arterial anatomy revisited: digital subtraction angiography performed in 600 patients. *Radiology.* 2002;224:542-547.
17. Flux G, Bardies M, Monsieurs M, Savolainen S, Strands SE, Lassmann M. The impact

- of PET and SPECT on dosimetry for targeted radionuclide therapy. *Z Med Phys.* 2006;16:47-59.
18. Patel CN, Chowdhury FU, Scarsbrook AF. Hybrid SPECT/CT: the end of "unclear" medicine. *Postgrad Med J.* 2009;85:606-613.
 19. Hamami ME, Poeppel TD, Müller S, et al. SPECT/CT with 99mTc-MAA in radioembolization with Y90 microspheres in patients with hepatocellular cancer. *J Nucl Med.* 2009;50:688-692.
 20. Ahmadzadehfah H, Sabet A, Biermann K, et al. The significance of 99mTc-MAA SPECT/CT liver perfusion imaging in treatment planning for Y90-microsphere selective internal radiation treatment. *J Nucl Med.* 2010;51:1206-1212.
 21. Gulec SA, Mesoloras G, Dezarn WA, McNeillie P, Kennedy AS. Safety and efficacy of Y90 microsphere treatment in patients with primary and metastatic liver cancer: the tumor selectivity of the treatment as a function of tumor to liver flow ratio. *J Transl Med.* 2007;5:15-24.
 22. Flamen P, Vanderlinden B, Delatte P, et al. Multimodality imaging can predict the metabolic response of unresectable colorectal liver metastases to radioembolization therapy with Yttrium-90 labeled resin microspheres. *Phys Med Biol.* 2008;53:6591-6603.
 23. Campbell JM, Wong CO, Muzik O, Marples B, Joiner M, Burmeister J. Early dose response to yttrium-90 microsphere treatment of metastatic liver cancer by a patient-specific method using single photon emission computed tomography and positron emission tomography. *Int J Radiat Oncol Biol Phys.* 2009;74:313-320.
 24. Ho S, Lau WY, Leung TW, et al. Partition model for estimating radiation doses from yttrium-90 microspheres in treating hepatic tumours. *Eur J Nucl Med.* 1996;23:947-952.
 25. Ho S, Lau WY, Leung TW, Chan M, Johnson PJ, Li AK. Clinical evaluation of the partition model for estimating radiation doses from yttrium-90 microspheres in the treatment of hepatic cancer. *Eur J Nucl Med.* 1997;24:293-298.
 26. Sirtex Medical Limited, New South Wales, Australia. Sirtex Medical training manual (version TRN-US-03, Sirtex.com). Undated.
 27. Gulec SA, Mesoloras G, Stabin M. Dosimetric techniques in Y90-microsphere therapy of liver cancer: The MIRD equations for dose calculations. *J Nucl Med.* 2006;47:1209-1211.
 28. Salem R, Lewandowski RJ, Gates VL et al. Research reporting standards for radioembolization of hepatic malignancies. *J Vasc Interv Radiol.* 2011;22:265-278.
 29. National Cancer Institute. Common Terminology Criteria for Adverse Events version 4.03. U.S. National Institutes of Health. June 14, 2010.
 30. Duke E, Deng J, Ibrahim SM. Agreement between competing imaging measures of response of hepatocellular carcinoma to yttrium-90 radioembolization. *J Vasc Interv Radiol.* 2010;21:515-521.
 31. Stabin MG, Sharkey RM, Siegel JA. RADAR commentary: evolution and current status of dosimetry in nuclear medicine. *J Nucl Med.* 2011;52:1156-1161.
 32. Van Hazel G, Blackwell A, Anderson J, et al. Randomised phase 2 trial of SIR-Spheres plus fluorouracil/leucovorin chemotherapy versus fluorouracil/leucovorin chemotherapy alone in advanced colorectal cancer. *J Surg Oncol.* 2004;88:78-85.
 33. Gates VL, Esmail AA, Marshall K, Spies S, Salem R. Internal pair production of Y90 permits hepatic localization of microspheres using routine PET: proof of concept. *J Nucl Med.* 2011;52:72-76.

34. Kennedy A, Dezarn W, Weiss A. Patient specific 3D image-based radiation dose estimates for Y90 microsphere hepatic radioembolization in metastatic tumors. *J Nucl Med Radiat Ther.* 2011;2:1-8.
35. Gulec SA, Szejnberg ML, Siegel JA. Hepatic structural dosimetry in (90)Y microsphere treatment: a Monte Carlo modeling approach based on lobular microanatomy. *J Nucl Med.* 2010;51:301-310.
36. Cremonesi M, Ferrari M, Bartolomei M. Radioembolization with Y90-microspheres: dosimetric and radiobiological investigation for multi-cycle treatment. *Eur J Nucl Med Mol Imaging.* 2008;35:2088-2096.